Available online at www.sciencedirect.com
ScienceDirect
Applied Radiation and Isotopes 64 (2006) 1186–1192
Applied Radiation and Isotopes
www.elsevier.com/locate/apradiso

Application of Monte Carlo simulation to the prediction of extrapolation curves in the coincidence technique

Mauro S. Dias[a,*], Mauro N. Takeda[b], Marina F. Koskinas[a]

[a]*Instituto de Pesquisas Energéticas e Nucleares: IPEN/CNEN-SP, Av. Prof. Lineu Prestes 2242, 05508-000, São Paulo, SP, Brazil*
[b]*Universidade Santo Amaro, UNISA, Rua Prof. Enéas da Siqueira Neto 340, 04829-300, São Paulo, SP, Brazil*

Abstract

A technique for simulating all detection processes in a $4\pi(\beta,e,X)$–γ coincidence system by means of the Monte Carlo technique is described. This procedure yields a more realistic behaviour of the extrapolation curve as compared to the usual polynomial fit. The present paper describes its application to the standardisation of a typical pure beta emitter, namely ^{35}S, by the efficiency tracing technique, and an EC-gamma radionuclide, namely ^{133}Ba. The calculated extrapolations were compared to experimental values obtained at the IPEN.

Keywords: Monte Carlo; ^{35}S; ^{60}CO; ^{133}Ba; Coincidence; Standardisation

1. Introduction

In $4\pi\beta$–γ standardisation, it is usually necessary to design the experimental conditions in order to optimise measurements and therefore minimise uncertainty in the resulting activity. Usually, this value is obtained by the Extrapolation Method (Baerg, 1973), changing the $4\pi\beta$ detector efficiency and extrapolating to 100% efficiency.

One critical condition to be set beforehand is the energy interval chosen for the gamma-ray channel. If the decay scheme is simple the selection is straightforward, however, for complex decay radionuclides this task becomes more difficult because pulses from different gamma-rays events may fall into the selected window. Moreover, when efficiency is not close to 100%, the curve shape in the extrapolation region may not be well defined, leading to ambiguities as shown recently in the literature (Morita et al., 2005). For the case of pure beta standardisation, where the efficiency tracing technique is usually applied, the behaviour of the extrapolation curve depends on the ratio between beta efficiencies of selected pure beta emitter and tracer radionuclides.

Usually for planning purposes, an analytical estimate of the extrapolation curve may be performed, taking into account the decay scheme information but without considering detailed detection characteristics for all radiations. The present approach is based on Monte Carlo simulation of all detection processes in a $4\pi\beta$–γ coincidence system to allow predicting the extrapolation curve with better accuracy. In this methodology, information contained in the decay scheme is used for determining the contribution of all radiations emitted by the selected radionuclide to the measured spectra of each detector. This simulation yields the shape of the coincidence spectrum, allowing the choice of suitable gamma-ray energies for which the activity can be obtained with maximum accuracy. Detailed characteristics of the LMN coincidence system are taken into account in order to perform calculation as realistically as possible.

In a previous work ^{134}Cs, a typical beta-gamma emitter, was considered (Takeda et al., 2004a). The present paper describes its application to the standardisation of ^{35}S, a typical pure beta emitter, by the efficiency tracing technique, and ^{133}Ba a typical EC-gamma radionuclide of complex decay scheme.

*Corresponding author. Fax: +55 011 3816 9188.
E-mail address: msdias@ipen.br (M.S. Dias).

0969-8043/$ - see front matter © 2006 Elsevier Ltd. All rights reserved.
doi:10.1016/j.apradiso.2006.02.019

2. Methodology

2.1. Coincidence equations

2.1.1. Efficiency tracing technique

The standardisation of pure beta emitters is usually performed by the efficiency tracing technique (ICRU, 1994). In this procedure a convenient beta-gamma emitter is used as tracer and mixed to the pure beta solution. The general coincidence equations applicable to this technique may be given by

$$N_\beta = N_{0P}\varepsilon_{\beta P} + N_{0P}\sum_{i=1}^{m} a_i \left\{ \varepsilon_{\beta_i} + (1-\varepsilon_{\beta_i})\sum_{j=1}^{n} b_{ij} \times \frac{\alpha_{ij}\left[\varepsilon_{CE_{ij}} + (1-\varepsilon_{CE_{ij}})\varepsilon_{(X,A)_{ij}}\right] + \varepsilon_{\beta\gamma_{ij}}}{1+\alpha_{ij}} \right\}_T, \quad (1)$$

$$N_{\gamma T} = N_{0T}\left(\sum_{i=1}^{m} a_i \sum_{j=1}^{n} b_{ij}\varepsilon_{\gamma_{ij}} \frac{1}{1+\alpha_{ij}}\right)_T, \quad (2)$$

$$N_{cT} = N_{0T} \times \left\{ \sum_{i}^{m} a_i \left[\varepsilon_{\beta_i} \sum_{j=1}^{n} b_{ij}\varepsilon_{\gamma_{ij}} \frac{1}{1+\alpha_{ij}} + (1-\varepsilon_{\beta_i}) \sum_{j=1}^{n} b_{ij}\varepsilon_{C_{ij}} \frac{1}{1+\alpha_{ij}} \right] \right\}_T. \quad (3)$$

Thus,

$$\frac{N_\beta N_\gamma}{N_c} = N_{0P}\varepsilon_{\beta P}\frac{N_\gamma}{N_c} + N_{0T}\left\{ \frac{\sum_{i=1}^{m} a_i \left\{ \varepsilon_{\beta_i} + (1-\varepsilon_{\beta_i})\sum_{j=1}^{n} b_{ij} \frac{\alpha_{ij}[\varepsilon_{CE_{ij}} + (1-\varepsilon_{CE_{ij}})\varepsilon_{(X,A)_{ij}}] + \varepsilon_{\beta\gamma_{ij}}}{1+\alpha_{ij}} \right\} \sum_{i=1}^{m} a_i \sum_{j=1}^{n} b_{ij}\varepsilon_{\gamma_{ij}} \frac{1}{1+\alpha_{ij}}}{\sum_{i}^{m} a_i \left[\varepsilon_{\beta_i} \sum_{j=1}^{n} b_{ij}\varepsilon_{\gamma_{ij}} \frac{1}{1+\alpha_{ij}} + (1-\varepsilon_{\beta_i}) \sum_{j=1}^{n} b_{ij}\varepsilon_{C_{ij}} \frac{1}{1+\alpha_{ij}} \right]} \right\}_T, \quad (4)$$

where P and T indexes stand for pure and beta-gamma emitters, respectively; N_β, N_γ and N_c are beta, gamma and coincidence counting rates, respectively; N_0 is the disintegration rate; a_i and b_{ij} are the intensity per decay of the ith beta transition and relative intensity of the jth transition with respect to the ith transition; n is the number of daughter transitions following the ith beta transition; m is the number of beta transitions; ε_{β_i} is the beta efficiency associated to ith beta transition; $\varepsilon_{\gamma_{ij}}$ and $\varepsilon_{\beta\gamma_{ij}}$ are gamma detection efficiency and gamma efficiency of beta detector, respectively, associated to ijth transition; $\varepsilon_{CE_{ij}}$ and $\varepsilon_{(X,A)_{ij}}$ are conversion electron detection efficiency and electron Auger or X-ray detection efficiency, respectively, associated to ijth transition, and $\varepsilon_{C_{ij}}$ and α_{ij} are the gamma–gamma coincidence detection efficiency and total internal conversion coefficient of the ijth transition.

A measure of the beta efficiency may be given by

$$\frac{N_c}{N_\gamma} = \frac{\sum_{i}^{m} a_i \left[\varepsilon_{\beta_i} \sum_{j=1}^{n} b_{ij}\varepsilon_{\gamma_{ij}} \frac{1}{1+\alpha_{ij}} + (1-\varepsilon_{\beta_i}) \sum_{j=1}^{n} b_{ij}\varepsilon_{C_{ij}} \frac{1}{1+\alpha_{ij}} \right]}{\sum_{i=1}^{m} a_i \sum_{j=1}^{n} b_{ij}\varepsilon_{\gamma_{ij}} \frac{1}{1+\alpha_{ij}}}. \quad (5)$$

In the special cases where the total energy absorption peak in the gamma channel can be selected as window for a single gamma-ray line (with intensity per decay b and conversion coefficient α), gamma–gamma coincidences are eliminated ($\varepsilon_{C_{ij}} = 0$) and Eqs. (4) and (5) can be simplified:

$$\frac{N_\beta N_\gamma}{N_c} = N_{0P}\varepsilon_{\beta P}\frac{N_\gamma}{N_c} + N_{0T} \times \left\{ 1 + b\frac{(1-\varepsilon_\beta)}{\varepsilon_\beta} \frac{\alpha[\varepsilon_{CE} + (1-\varepsilon_{CE})\varepsilon_{(X,A)}] + \varepsilon_{\beta\gamma}}{1+\alpha} \right\}_T \quad (6)$$

and

$$\frac{N_c}{N_\gamma} = \varepsilon_{\beta T}, \quad (7)$$

where

$$\varepsilon_{\beta T} = \left\{ \sum_{i=1}^{m} a_i \varepsilon_{\beta_i} \right\}_T.$$

For a simple decay scheme such as ^{60}Co, the second term of Eq. (4) is almost constant because the conversion coefficients and $\varepsilon_{\beta\gamma}$ values for ^{60}Co are small. For this reason, the behaviour of this equation depends mainly on the ratio between pure beta emitter and tracer efficiencies. The first purpose of the present work was to simulate Eqs. (4) and (5) by the Monte Carlo method for ^{35}S + ^{60}Co mixture and compare to experimental results obtained at LMN.

2.1.2. Electron capture radionuclides

For EC emitters standardised by the coincidence method, the corresponding equation is similar to (4) except that the first term is omitted and ε_β is changed to ε_{EC}. The latter symbol corresponds to the 4π detector efficiency for Auger electrons and X-rays coming from electron capture events. The present work compares the simulation of Eqs. (4) and (5) by Monte Carlo with the experimental results obtained at the LMN for ^{133}Ba.

3. Monte Carlo simulation

3.1. Efficiency tracing

The deposited energy spectra were determined for monoenergetic electron and photons as a function of the energy by means of the MCNP-4C code (ORNL, 2001), taking into account detailed design information of the LMN $4\pi(\beta,X)$–γ coincidence system (Hilário, 2002). In the case of the 4π proportional counter, electrons from 100 eV to 3 MeV were considered; for NaI(Tl) photons from 10 keV

to 4 MeV were considered. The beta spectral shapes were estimated by the Fermi Theory of β Decay (Evans, 1955).

A Monte Carlo code called ESQUEMA1 (Takeda et al., 2004a, b) was written in order to follow the decay scheme, from the precursor nucleus to the ground state of the daughter nucleus. The flow diagram of this code is shown in Fig. 1. This code makes use of electron and photon deposited energy spectra tables previously calculated by MCNP-4C.

A probability function was derived from the beta spectrum shape, and the emitted beta energy was sampled by a random number. After the electron energy is determined, a random direction is chosen and the path in the absorber is compared to the electron range. If the electron crosses the absorber, its residual energy is computed and the deposited energy taken from the table. This procedure was used to avoid a multitude of deposited energy tables that would be necessary in order to cover all absorber combinations.

Following the decay scheme, the choice between the gamma or conversion electron transition was made by sampling another random number. When the gamma-ray is detected the deposited energy is sampled from the table. If the gamma transition was detected in coincidence with a beta event, a count in the coincidence spectrum was registered, in the same channel position as the gamma event. In the case where the conversion electron was detected in coincidence with the beta particle, a count was registered in the beta spectrum, corresponding to the sum of both deposited energies. The present version of the code allows selection by changing the cut-off of deposited energy in the $4\pi\beta$ detector and by applying absorbers on the radioactive source substrate. In this way it was possible to simulate variation in beta efficiency.

3.2. Electron capture standardisation

Another Monte Carlo code called ESQUEMA2 was developed. This code is similar to ESQUEMA1 except the beta transition procedure which was modified for Electron Capture events. Initially, the electron shell is chosen by a random number according to transition probabilities $(P_K, P_L, \ldots)$ taken from the literature. The choice between X-ray or Auger electron emission is performed sampling a random number according to the shell fluorescence yield $(w_K, w_{L,} \ldots)$. The X_K ray energy emitted for a KX transition $(X = L, M, N, \ldots)$ is given by

$$E_{KX} = E_K - E_X. \tag{8}$$

The Auger Electron energy is given by

$$E_{AK} = E_K - E_X - E_Y, \tag{9}$$

where E_K, E_X, E_Y are the binding energies of the K, X and Y electron shells, respectively. In the present version, the correction to account for the difference between excited and ground state binding energies of the atom has been neglected. After the Auger electron energy is determined, a random direction is chosen and the path in the absorber is compared to the electron range. If the electron crosses the absorber, its residual energy is computed and the deposited energy taken from the table.

4. Experimental setup

4.1. Efficiency tracing

The standardisation of $^{35}S + {}^{60}Co$ mixture was performed by means of a conventional 4π(PC)β–γ coincidence system, consisting of 4π proportional counter filled with P-10 gas mixture at 0.1 MPa, coupled to a pair of 3 in × 3 in NaI(Tl) crystals. A detailed description of this detection system is given elsewhere (Hilário, 2002). All pulses above the noise threshold (0.7 keV) were measured in the beta channel. The gamma-rays were gated via a discrimination window, covering the total absorption peaks of 1173 and 1332 keV, respectively.

Two types of radioactive sources to be measured in the 4π(PC)β–γ system were prepared: pure ^{60}Co and $^{35}S + {}^{60}Co$ mixed sources. Known aliquots of the radioactive solution were dropped on 20 $\mu g\,cm^{-2}$ thick Collodion film, previously coated with a 10 $\mu g\,cm^{-2}$ thick gold layer on each side, to render it conductive. A seeding agent (CYASTAT) was used for improving the deposit uniformity and the sources were dried in warm (40 °C) nitrogen jet flow. The accurate source mass determination was performed using a Sartorius MC21S electronic balance by the pycnometre technique (Campion, 1959). The variation in the efficiency was achieved by placing external Collodion or aluminium absorbers over or under the radioactive sources.

4.2. Electron capture standardisation

The same 4π(PC)β–γ coincidence system described in the previous section was used for the standardisation of ^{133}Ba. The radioactive solution was sent by the BIPM to the LMN of IPEN as part of an international comparison held in 1984 (Rytz, 1985). The 4π(PC) detector bias was +2050 V and the discrimination lower level set to cut off noise at 0.91 keV. The gamma-ray discrimination window was set to cover the energy range between 222 and 420 keV, approximately. The radioactive source preparation followed the same procedure as described for ^{60}Co and the detection efficiency was changed in a similar way.

4.3. Comparison between experiment and simulated extrapolation curves

Least-squares fitting has been performed in order to provide the extrapolated activity value N_0 combining experimental and simulated data. The corresponding chi-square statistic was given by

$$\chi^2 = (\vec{y}_{exp} - N_0\vec{y}_{MC})^T V^{-1}(\vec{y}_{exp} - N_0\vec{y}_{MC}), \tag{10}$$

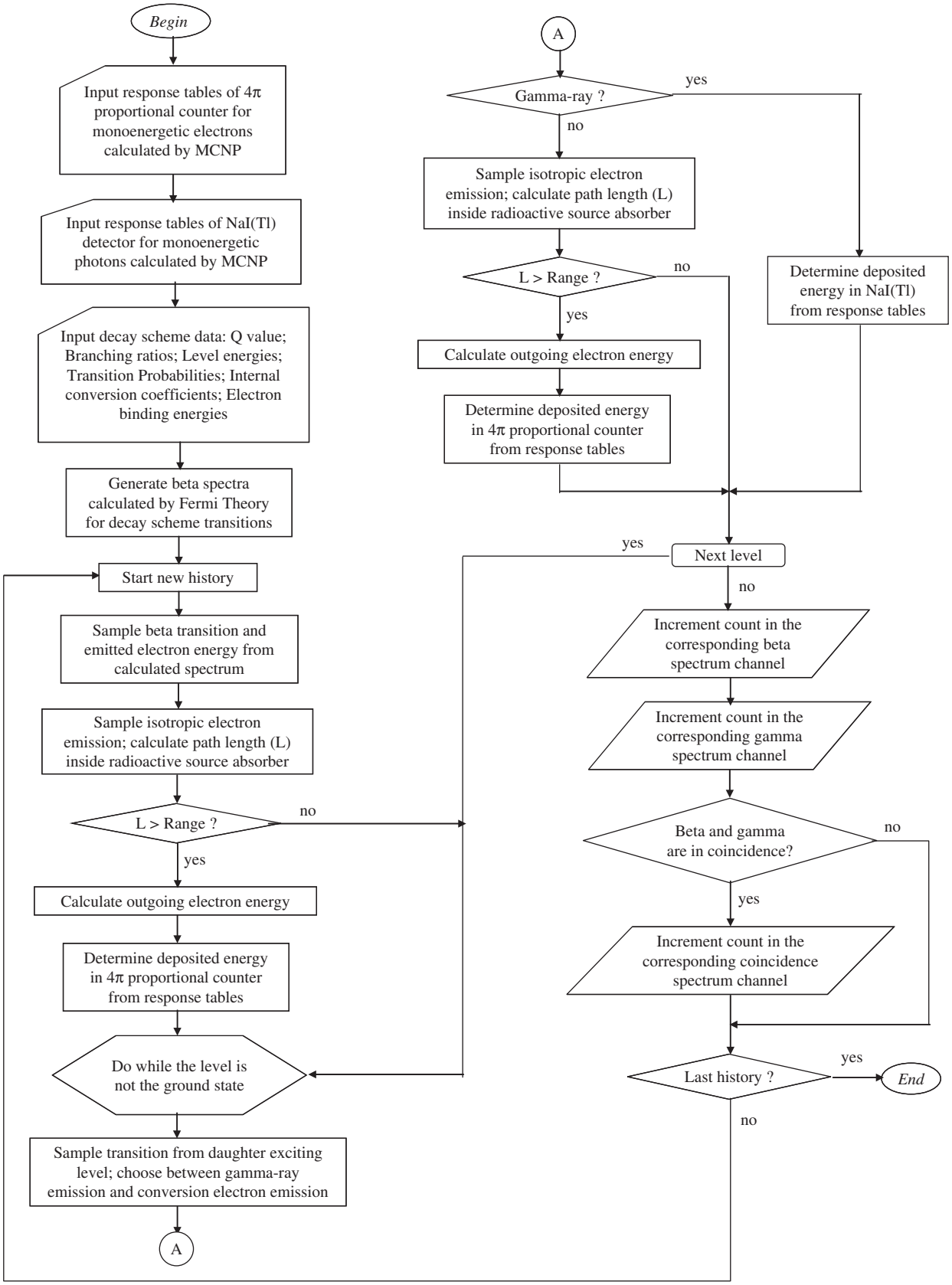

Fig. 1. Flow diagram of code ESQUEMA1.

where $\vec{y}_{exp}$ is the experimental vector of $N_\beta N_\gamma/N_c$; $\vec{y}_{MC}$ is the $N_\beta N_\gamma/N_c$ vector calculated by Monte Carlo for unitary activity; N_0 is the specific activity of the radioactive solution; V is the total covariance matrix, including both experimental and calculated uncertainties, and T stands for matrix transposition.

A series of simulated values were calculated for a wide range of beta efficiency parameter in small bin intervals. The $\vec{y}_{MC}$ values used in Eq. (10) correspond to the same efficiency obtained experimentally. In the case of efficiency tracing technique, the tracer activity has been subtracted from $\vec{y}_{exp}$ before performing the fit.

5. Results and discussion

Fig. 2 shows the behaviour of $N_\beta N_\gamma/N_c$ curve as a function of efficiency parameter $(1-\varepsilon_\beta)/\varepsilon_\beta$ (where ε_β corresponds to N_c/N_γ), for ^{35}S. The closed circles correspond to experimental results obtained by placing external absorbers above and below the radioactive sources. The open circles correspond to values predicted by the Monte Carlo method. In this simulation, the beta efficiency variation was achieved by changing the absorber thickness placed over and under the radioactive source. As can be seen, there is good agreement between the experimental and calculated curve shapes within the statistical uncertainty and indicates a non-linear behaviour. The negative slope is expected because the ^{35}S beta end-point energy is smaller than the corresponding value for ^{60}Co. The resulting ^{35}S activity obtained by least-squares fitting according to Eq. (10) was 39.5(2) kBq g^{-1}. Additional fittings were performed using first and second degree polynomials, and the results were 38.8(3) and 40.0(6) kBq g^{-1}, respectively. The Monte Carlo points lie between the two polynomial curves indicating the expected behaviour of a more realistic curve. The uncertainty components involved in these procedures are shown in Table 1. The main uncertainty component for the polynomial functions comes from the least-squares fitting procedure, and, for the Monte Carlo methodology, it comes from the tracer gamma-ray background.

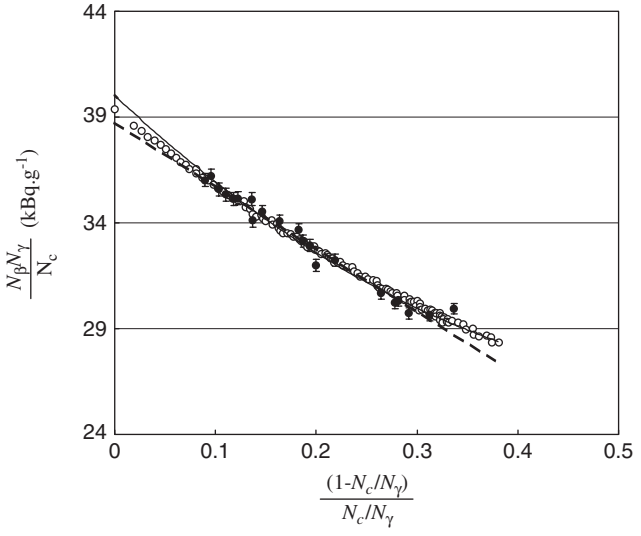

Fig. 2. Behaviour of $N_\beta N_\gamma/N_c$ as a function of efficiency parameter $(1-N_c/N_\gamma)/(N_c/N_\gamma)$ for ^{35}S. Closed circles correspond to experimental data and open circles to Monte Carlo calculation. The dashed and continuous curves correspond to first and second degree polynomial fittings, respectively.

Table 1
Average uncertainty components per data point and combined uncertainties involved in ^{35}S activity determination ($k = 1$)

Source of uncertainty	Value (%)
Counting statistics	0.16
Weighing (^{35}S)	0.10
Weighing (^{60}Co)	0.11
Dead time	<0.1
Resolving time	<0.1
Background	0.27
Tracer activity	0.16
Monte Carlo statistics	0.21
Polynomial fitting (first degree)	0.53
Combined uncertainty (polynomial fitting—first degree)	0.66
Polynomial fitting (second degree)	1.51
Combined uncertainty (polynomial fitting—second degree)	1.56
Fitting according to Eq. (10)	0.21
Combined uncertainty (Eq. (10))	0.44

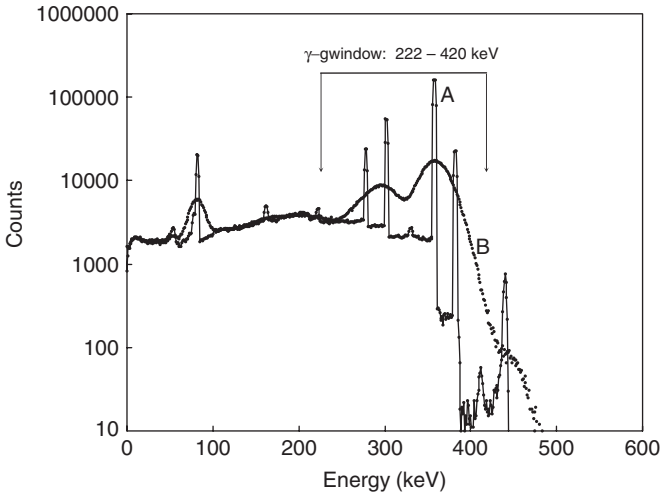

Fig. 3. Gamma-ray spectra from ^{133}Ba simulated by Monte Carlo. Spectrum A is without resolution effects. Spectrum B includes resolution, matching experimental spectrum at 661.6 keV.

Fig. 3 shows two ^{133}Ba gamma-ray spectra from the NaI(Tl) simulated by Monte Carlo according to the geometry of $4\pi\beta$(PC)–γ system. Spectrum A does not incorporate resolution effects and shows the contribution of all gamma lines. Spectrum B incorporates NaI(Tl) resolution matching the experimental spectrum at 661.6 keV corresponding to ^{137}Cs gamma energy. The resolution at other energies follows the $1/\sqrt{E}$ law (Knoll, 1989). As can be seen, the window at 356 keV, besides the main gamma line of 356.01 keV (63.64%), incorporates

three other gamma lines, namely: 276.40 keV (7.57%), 302.85 keV (19.15%) and 383.85 keV (9.12%) (BIPM, 2004). The last peak comes from cascade summing of 356.01 and 53.16 keV gamma lines. Since the transitions of 53.16 and 81.00 keV have high internal conversion coefficients, a part of beta efficiency comes from detection of these conversion electrons in coincidence with cascade gamma-rays.

Fig. 4 shows the behaviour of $N_\beta N_\gamma/N_c$ curve as a function of efficiency parameter $(1-\varepsilon_\beta)/\varepsilon_\beta$ for the case of ^{133}Ba. The closed circles correspond to experimental results and the open circles correspond to values predicted by the Monte Carlo method, normalised by the activity value. The full line corresponds to a second degree polynomial. There is a good agreement between the experimental shape and the one calculated by Monte Carlo. The ^{133}Ba activity was obtained by least-squares fit of Eq. (10) and resulted 1160.0(12) Bq g^{-1}. This value is in excellent agreement with the value 1159.9(15) Bq g^{-1} obtained using a second degree polynomial and with the average value obtained in the comparison, 1160.8(42) Bq g^{-1} (Rytz, 1985). The partial uncertainties involved in the present methodology for ^{133}Ba are shown in Table 2. The main uncertainty component for the polynomial function comes from the least-squares fitting procedure and for the Monte Carlo methodology it comes from the counting statistics and weighing procedure.

For polynomial fittings, the uncertainty confidence band enlarges as the curve departs from the experimental values. In this case, the extrapolated value usually shows larger uncertainty as compared to interpolated values. In the Monte Carlo approach, the activity value is obtained from Eq. (10), which does not involve extrapolations, and this may explain the lower uncertainty obtained in the Monte Carlo methodology.

A complete account for all uncertainties involved in the Monte Carlo procedure is underway and shall consider several factors included in the simulation, such as:

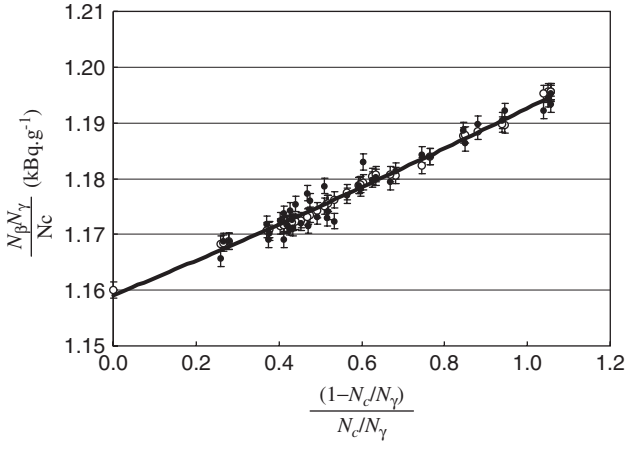

Fig. 4. Behaviour of $N_\beta N_\gamma/N_c$ as a function of efficiency parameter $(1-N_c/N_\gamma)/(N_c/N_\gamma)$ for ^{133}Ba. Closed circles correspond to experimental data and open circles to Monte Carlo calculation. The full line corresponds to second degree polynomial fitting.

Table 2
Average uncertainty components per data point and combined uncertainties involved in ^{133}Ba activity determination ($k = 1$)

Source of uncertainty	Value (%)
Counting statistics (per data point)	0.05
Weighing	0.05
Dead time	<0.01
Resolving time	<0.01
Adsorption	0.04
Background	0.04
Monte Carlo statistics	0.14
Polynomial fitting (second degree)	0.13
Combined uncertainty (polynomial fitting)	0.16
Fitting according to Eq. (10)	0.03
Combined uncertainty (Eq. (10))	0.10

detection geometry, decay scheme and response functions. However, previous (Takeda et al., 2004a) and present works show that this approach yields extrapolation curve shapes close to experimental points, for different kinds of radionuclide decay schemes, allowing confidence in the procedure.

It can be concluded that the Monte Carlo simulation yielded extrapolation curves in close agreement with experiment for the efficiency tracing technique as well as for EC radionuclide decay and it may show lower uncertainty as compared to polynomial fitting. Since this approach is based on realistic behaviour, it can be a powerful tool for obtaining the extrapolated value, mainly when the efficiency is not close to 100%, which is an undesired situation that can lead to ambiguous results as seen in the literature (Morita et al., 2005).

Acknowledgements

The authors are indebted to Mrs. Eliane Pocobi for the careful sample preparations and to the Radiopharmaceutical Centre of IPEN for supplying the ^{35}S solution.

References

Baerg, A.P., 1973. The efficiency extrapolation method in coincidence counting. Nucl. Instrum. Methods 112, 143–150.

BIPM, 2004. Monographie BIPM-5, Table of Radionuclides, CIPM/CCRI, November 2004 (CD-ROM).

Campion, P.J., 1959. The standardisation of radioisotopes by beta-gamma coincidence method using high efficiency detectors. Int. J. Appl. Radiat. Isot. 4, 232–248.

Evans, R.D., 1955. The Atomic Nucleus. McGraw-Hill Book Company, New York, p. 548.

Hilário, K.A.F., 2002. Development of methods for activity determination for radionuclides with double decay emission β^-–β^+/electron capture—application to the standardisation of ^{192}Ir, ^{152}Eu and ^{186}Re. Ph.D. Thesis, University of São Paulo, Brazil (in Portuguese).

ICRU, 1994. International Commission on Radiation Units and Measurements. Particle Counting in Radioactivity Measurements. ICRU Publ., Bethesda, MD, USA. November (ICRU-Report 52).

Knoll, G.F., 1989. Radiation Detection and Measurement, second ed. Wiley, New York.

Morita, K., Miyahara, H., Ogata, Y., Katoh, K., 2005. Emission probability measurement of γ-ray of ^{105}Rh. Nucl. Instrum. Methods A 540, 324–327.

ORNL, 2001. Monte Carlo N-Particle Transport Code System, MCNP4C, RSICC Computer Code Collection, Oak Ridge National Laboratory. Report CCC-700.

Rytz, A., 1985. International comparison of activity measurements of a solution of ^{133}Ba (March 1984). Rapport BIPM-85/11.

Takeda, M.N., Dias, M.S., Koskinas, M.F., 2004a. Application of Monte Carlo simulation ^{134}Cs standardisation by means of $4\pi\beta$–γ coincidence system. In: Proceedings of Nuclear Science Symposium, IEEE Conference, Rome (CD-ROM).

Takeda, M.N., Dias, M.S., Koskinas, M.F., 2004b. Monte Carlo simulation of activity measurements by means of $4\pi\beta-\gamma$ coincidence system. Brazilian J. Phys. 34 (3A).